Rings of Earth Detected by Orbital Debris Radar

R. Goldstein
Telecommunications Science and Engineering Division

L. Randolph
TDA Engineering Office

Small particles moving at an orbital velocity of 7.6 kilometers per second can present a considerable hazard to human activity in space. For astronauts outside of the protective shielding of their space vehicles, such particles can be lethal. The powerful radar at NASA's Goldstone Deep Space Communications Complex has been used to monitor such orbital debris. This radar can detect metallic objects as small as 1.8 mm in diameter at 600 km altitude. The results of the preliminary survey show a flux (at 600 km altitude) of 6.4 objects per square kilometer per day of equivalent size of 1.8 mm or larger. Forty percent of the observed particles appear to be concentrated into two orbits. An orbital ring with the same inclination as the radar (35.1 degrees) is suggested. However, an orbital band with a much higher inclination (66 degrees) is also a possibility.

I. Orbital Debris

In support of Space Station Freedom's shielding design, NASA, through its Office of Space Tracking and Data Systems, has been obtaining orbital debris information from various sources. To augment these data, two experiments have been conducted by JPL to obtain information on debris less than 10 cm in diameter. The first experiment was conducted by Tommy Thompson of JPL and Donald Campbell of Cornell University at the Arecibo Observatory in Puerto Rico, and was able to detect debris down to 5 mm in diameter. The second experiment, which is described here, utilized a radar of a shorter wavelength, which can thereby detect smaller particles.

II. The Radar

The radar used for this survey is at the Goldstone Deep Space Communications Complex. An X-band (8.5 GHz) radar transmitter connected to the 70-m dish antenna, DSS 14, was used to illuminate the orbital particles with 3-ms pulses (with an 8-ms repetition period) of otherwise unmodulated microwave energy. A receiver was connected

to a smaller 26-m antenna, DSS 13, located 21.6 km from the transmitter. The antennas were pointed so that the beams intersected 600 km above the midpoint between the two antennas. The radar parameters were:

Transmitter power = 340 kW (average)

Transmitter antenna gain = 2.3×10^7 (over isotropic)

Receiver antenna area = 191 m^2 (effective)

System noise temperature = 24.3 K

Wavelength = 3.5 cm

Figure 1 shows the geometry of the experiment. The cross-sectional area of the antenna beam intersection was 11.6 km^2. Particles in near circular orbits at 600 km altitude take 51 ms to traverse the beam intersection.

III. Observations

Two- to five-hour observation periods were scheduled on an irregular basis from March 22 to October 16, 1989. Altogether, 48 hours of data were collected over 15 separate days or nights.

IV. Signal Processing

Received signals were filtered to a bandwidth of 10 kHz and stored on digital magnetic tape. Subsequently, blocks of 3-ms duration were Fourier transformed and accumulated over 48 ms. The resulting power spectra were compared to a threshold to decide if there had been a "hit" or if there were only noise in the data.

The threshold was determined from a chi-squared distribution of 12 degrees of freedom such that, on average, there would be one false alarm per 5 hours (375,000 spectra). The resulting signal-to-noise ratio (3.87) corresponds to a radar cross section of 5.8×10^{-3} mm^2, which was chosen as the detection limit. At this wavelength, a metallic sphere of 1.8-mm diameter has this radar cross section.

The number of reported events was reduced by the expected number of false alarms. Thus, the reported flux is a lower limit; there must have been undetected small particles.

V. Data

The spectrograms for a representative event are shown in Fig. 2. Five spectrograms are plotted in a time sequence separated by 48 ms (the approximate time within the beam intersection). Line-of-sight velocity is the abscissa; relative power density is the ordinate. The line-of-sight velocity component of ± 88 m/sec corresponds to a frequency range of ±5 kHz. The signal-to-noise ratio for this event was 6.5, somewhat over the threshold and corresponding to a metallic sphere of 1.9-mm diameter.

Figure 3 is a cumulative distribution of all the particles detected in the survey, plotted according to radar cross section. Along the upper abscissa is the size of the equivalent metallic sphere of the same radar cross section. Note that the actual particles can be larger than those indicated (i.e., nonmetallic particles).

VI. Swarms

For most observation days, one or two events per hour were recorded. During some hours, however, the rate was as high as 15. What happened on those days to produce swarms of events?

Figure 4 gives the results of one such day. The time for each event is plotted against the line-of-sight velocity. The velocity is measured from the spectrogram and represents the Doppler shift generated by the (small) radial velocity of the object when it crossed the antenna beam. The signal-to-noise ratio of each event is marked on the figure. Within the accuracy of the velocity estimates, one straight line goes through most of the points. These separate events are, therefore, strongly related; they must have a common origin. However, during the hour-long lifetime of such a swarm, the Earth has rotated 15 degrees. How is it possible for this family of objects to remain so long in an antenna beam of only 315-m width at that altitude?

Figure 5 presents one answer: the objects are in a common orbit (a ring) that has the same inclination as the latitude of the radar. Then, the Earth's rotation carries the radar in a direction that is parallel to the putative ring. Such an hypothesis should be easy to test. All one needs to do is to repeat the experiment the next sidereal day, when the radar has rotated back under the ring. Unfortunately, the observation schedule has so far been too irregular, averaging only two tracks per month.

During the survey, six occasions were found where the velocity–time plots could be essentially connected by one straight line. For each of these occasions, the time of the zero crossing of the straight line is plotted against the day of the year on which it occurred. The result is given in Fig. 6.

A single straight line connects five of the six points. This indicates that the same orbit was observed five times. The slope of the line represents the precession of the orbit, which was 3.0 degrees per day. The orbit is prograde. The sixth point of Fig. 6 represents a second orbit; one observed only once. The velocity–time line for that swarm had the opposite slope from the other five.

The observed precession rate seems too low for an orbit of 35-degree inclination. It matches, instead, what one would expect for 66 degrees.

A second possibility is that of a satellite at the higher inclination that has broken up in orbit. The debris might then have spread into a band that would be in the Goldstone beam for the required hour.

The breakup must have been rather violent, since so many small particles were produced. Such a process would tend to randomize the Doppler shifts, which is contrary to the linear relationship which was found.

The dotted circle on Fig. 6 represents one day when observations were made at the correct time to see the swarm, but no swarm was seen. One that day, the receiver's circular polarization was reversed. Large, irregular objects and flake or wire shapes can reverse the sense of circular polarization. The observed swarm was not composed of these.

VII. Conclusions

From the observed average flux of 6.4 events/km^2/day, the expected time for a human-sized object to be hit is 214 years. The danger, however, appears to depend on location. Within the ring volume, the expected time drops to 59 years. And at the convergence point (if it exists) of the orbital band, the expected time is only 1.5 months. In any case, the situation is continually deteriorating as more and more debris is deposited into orbit. Furthermore, there is an undetermined, but apparently larger, flux of particles smaller than 1.8 mm that could pose a hazard.

Acknowledgments

The authors thank Don Kessler for helpful discussions about orbital dynamics, and the Goldstone crew for the many hours spent in preparing and running this experiment.

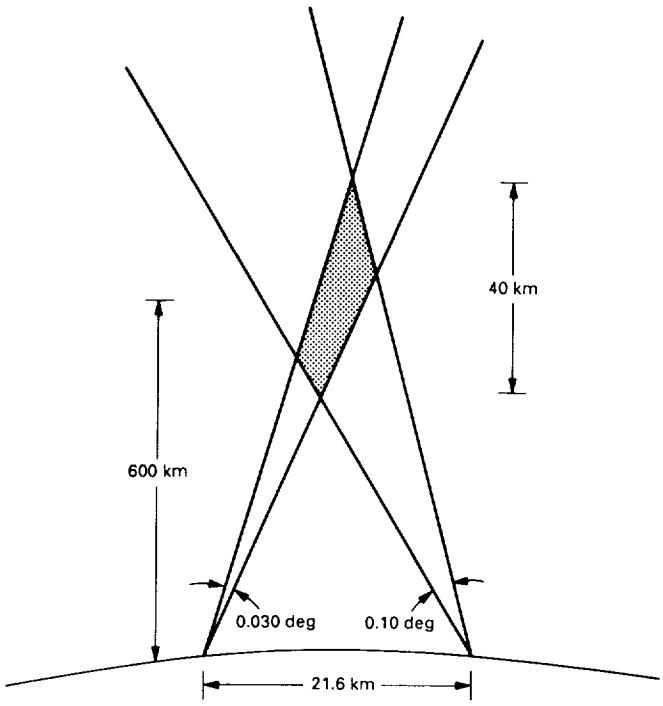

Fig. 1. The intersection of the two antenna beams. The common area of 11.6 km^2 was centered at an altitude of 600 km.

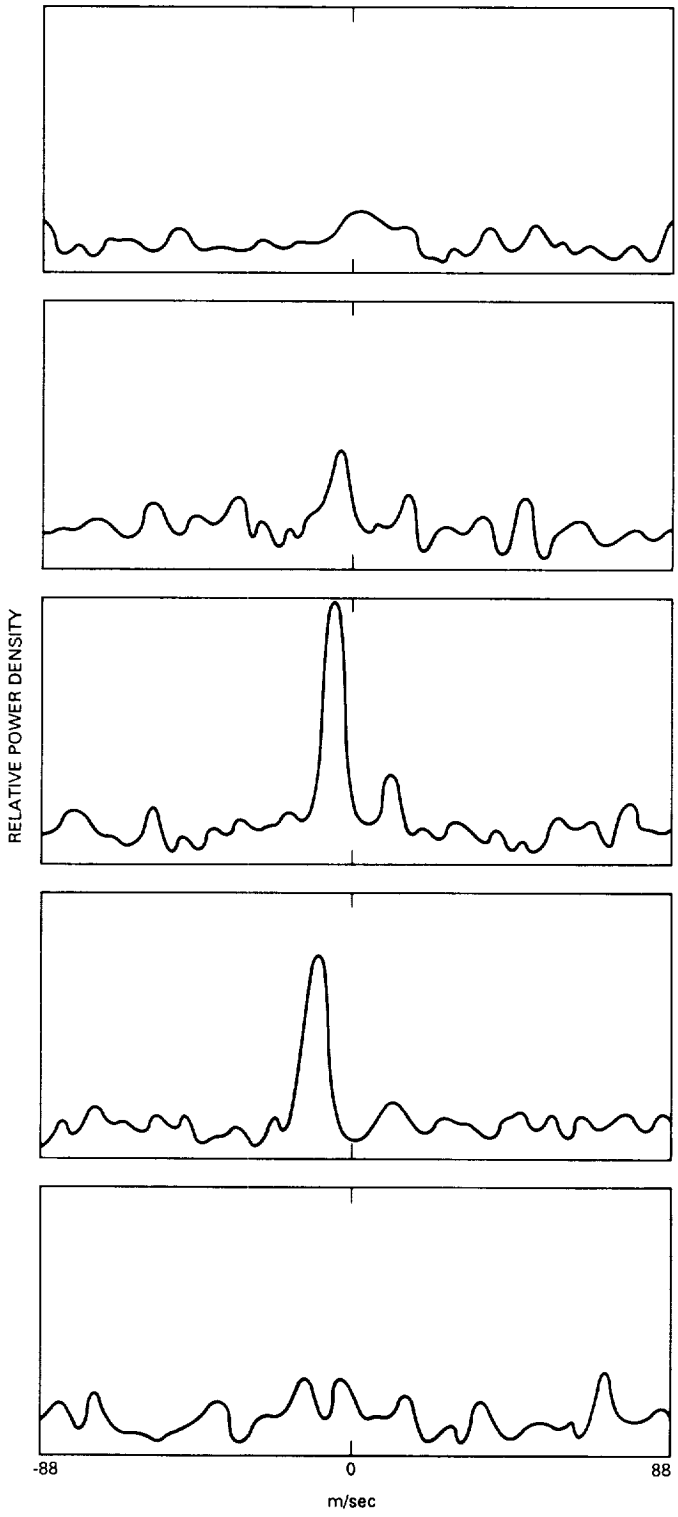

Fig. 2. Spectrograms separated in time by 48 ms. An object of equivalent diameter of 1.9 mm appears to have passed through the intersection of the two antenna beams.

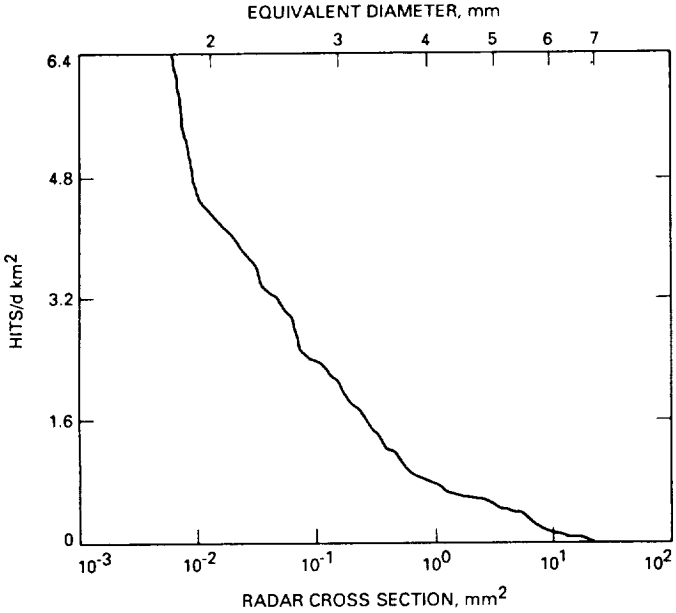

Fig. 3. Cumulative distribution for the flux of orbital debris. For each radar cross section, the plot gives the flux of particles of that cross section or larger.

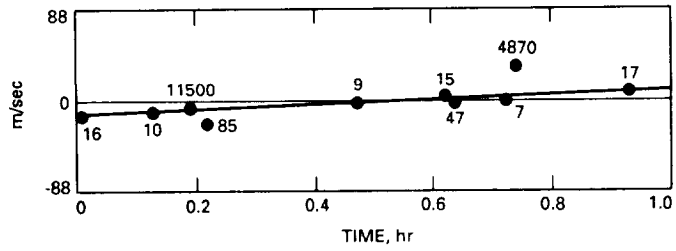

Fig. 4. Record of events during one hour on September 4, 1989. One straight line fits the data so well that the events must be related. Numbers indicate the signal-to-noise ratio.

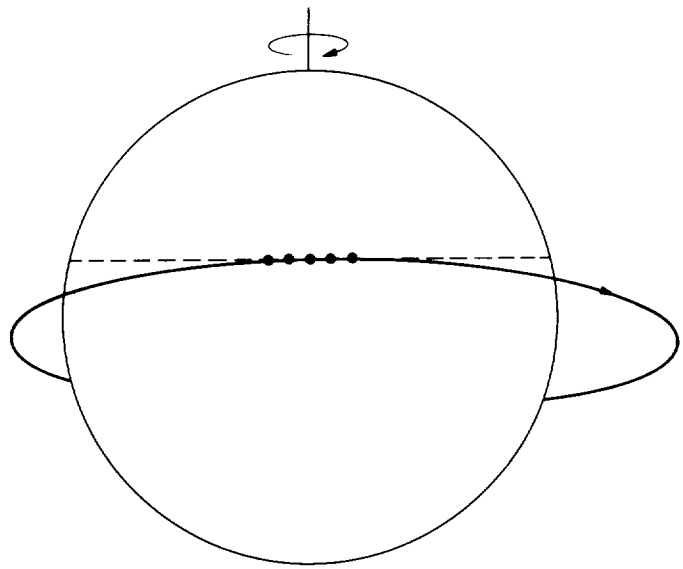

Fig. 5. Diagram showing how an antenna fixed to the rotating Earth can illuminate an orbital ring for an extended period of time.

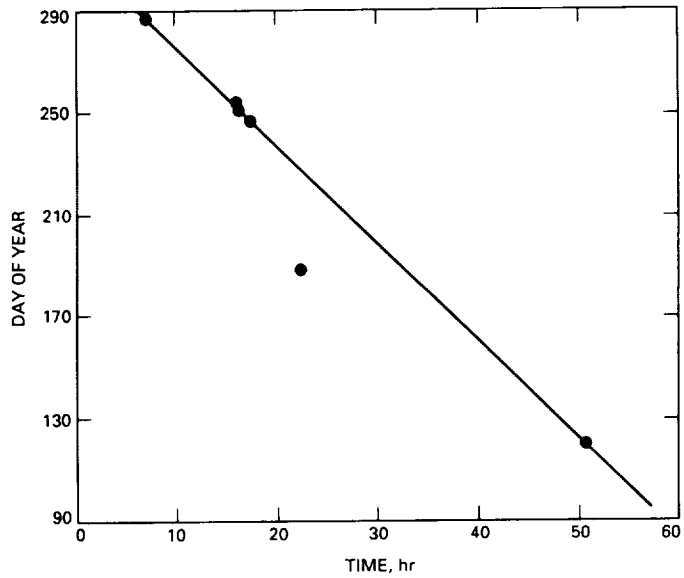

Fig. 6. Day-of-year versus time-of-day plot shows that five of the six observed swarms were repeat observations of the same orbital ring, precessed by 3.0 degrees per day.

Errata

The following tables were inadvertently left out of W. M. Folkner and M. H. Finger's article, "Photon Statistical Limitations for Daytime Optical Tracking," that appeared in the *Telecommunications and Data Acquisition Progress Report 42-99*, vol. July–September 1989, November 15, 1989:

Table 1. Characteristics of nominal astrometric tracking system

Receiver characteristics	
Aperture diameter d_r, m	1.0
Filter bandwidth $\Delta\lambda$, nm	100.0
Atmospheric transmission η_a	0.5
Obscuration factor η_{ra}	0.9
Optics efficiency η_{ro}	0.8
Filter transmission η_e	0.8
Detector efficiency η_d	0.5
Transmitter characteristics	
Laser power P, W	2.00
Laser wavelength λ, nm	532.00
Transmitter diameter d_t, m	0.30
Distance from Earth, au	10.00
Obscuration factor η_{ta}	0.71
Pointing efficiency η_{tp}	0.84
Optics efficiency η_{to}	0.65

Table 2. Integration times needed for photon statistical error to reach a specified angular accuracy, considering a star of magnitude m = 8 and a 2-W laser on the spacecraft. Several different filter bandpasses are considered. Note that the 0.03-nm filter has a different transmission efficiency.

Source	Star	Star	S/C	S/C	S/C
m_v or power	8	8	2 W	2 W	2 W
Bandpass, nm	100	1.0	100	1.0	0.03
Count rate, photons/s	6.8×10^5	6.8×10^3	2.6×10^4	2.6×10^4	2.6×10^4
Background rate, photons/s	2.6×10^9	2.6×10^7	2.6×10^9	2.6×10^7	3.8×10^5
T for 50 nrad, s (no background)	0.0099	0.99	0.26	0.26	0.52
T for 5 nrad, s (no background)	0.99	99	26	26	52
T for 50 nrad, s (with background)	38	3.8×10^5	2.6×10^4	260	15
T for 5 nrad, s (with background)	3.8×10^3	3.8×10^7	2.6×10^6	2.6×10^4	1.5×10^3